Identification of a novel antiviral micro-RNA targeting the NS1 protein of the H1N1 pandemic human influenza virus and a corresponding viral escape mutation

Laura Bavagnoli[a,1], Giulia Campanini[b,1], Maurizio Forte[a], Giorgia Ceccotti[a], Elena Percivalle[b], Silvia Bione[a], Antonella Lisa[a], Fausto Baldanti[b], Giovanni Maga[b,*]

[a] Institute of Molecular Genetics IGM-CNR "Luigi Luca Cavalli-Sforza", Via Abbiategrasso 207, 27100, Pavia, Italy
[b] Molecular Virology Unit, Microbiology and Virology Department, Fondazione IRCCS Policlinico San Matteo, 27100, Pavia, Italy

A B S T R A C T

The influenza A virus (IAV) NS1 protein is one of the major regulators of pathogenicity, being able to suppress innate immune response and host protein synthesis. In this study we identified the human micro RNA hsa-miR-1307-3p as a novel potent suppressor of NS1 expression and influenza virus replication. Transcriptomic analysis indicates that hsa-miR-1307-3p also negatively regulates apoptosis and promotes cell proliferation. In addition, we identified a novel mutation in the NS1 gene of A(H1N1)pdm09 strains circulating in Italy in the 2010-11 season, which enabled the virus to escape the hsa-miR-1307-3p inhibition, conferring replicative advantage to the virus in human cells. To the best of our knowledge, this is the first validation of suppression of IAV H1N1 NS1 by a human micro RNA and the first example of an escape mutation from micro RNA-mediated antiviral response for the A(H1N1)pdm09 virus.

1. Introduction

The pandemic swine-derived influenza A virus (IAV) A(H1N1)pdm09 is a multiple reassortant (Neumann et al., 2009) and currently the predominant circulating H1N1 influenza virus in humans. Phylogenetic and molecular studies provided evidence that, globally, the A(H1N1)pdm09 virus has evolved since the initial onset of the pandemic, with natural selection being driven by host adaptation and, subsequently, by immunological escape (Pan et al., 2010; Belanov et al., 2015; Su et al., 2015). In particular, a phylogenetic studies suggested that the genomic segment 8 of A(H1N1)pdm09, encoding for the NS1 and NS2 proteins, has been under positive selection during the first wave of the pandemic from April 2009 to May 2010 (Wang et al., 2013). Indeed, a number of aminoacidic substitutions in the NS1 gene have been reported to have accumulated during pandemic and post-pandemic circulation of A(H1N1)pdm09 viral strains, suggesting that the A(H1N1)pdm09 NS1 underwent significant evolution between the 2009–10 and 2010-11 seasons, giving rise to novel variants possibly correlating with higher fitness and increased pathogenicity for the human host (Otte et al., 2016; Clark et al., 2017).

The NS1 protein is one of the major regulators of IAV pathogenicity

and it is exclusively produced during infection in cells, without being incorporated into the new viral particles. It contains an RNA binding domain at its amino terminal and an effector domain at its carboxy terminal moieties, respectively. This latter protein segment contains the binding sites for several cellular proteins. Thanks to these interactions, NS1 can interfere with various cellular pathways including RNA processing and innate immunity interferon (IFN)-mediated response (Krug, 2015).

Phylogenetic analysis suggested that the A(H1N1)pdm09 virus was introduced in Italy through multiple importations in the spring of 2009. Founder effects in the post-pandemic period led then to the evolution of specific Italian clades (Zehender et al., 2012). The A(H1N1)pdm09 strains circulating in the second wave in Italy were associated to a higher incidence of severe symptoms with respect to the previous season (637,502 more cases or +13%), similarly to what has been observed in other European countries (Gasparini et al., 2013). The reasons behind the increased pathogenicity of second-wave pandemic A(H1N1)pdm09 strains are still incompletely understood, but strong evidence support a role for positive selection at different amino acid positions important for antigen recognition and immune escape (Zehender et al., 2012; Goka et al., 2014; Otte et al., 2016).

In the present study, we identified the nucleotide substitution C112A at codon 38 of the protein, which falls within the putative target site of the human micro RNA hsa-miR-1307-3p. We found that over-expression of hsa-miR-1307-3p in A549 cells reduced wild type NS1 expression and replication of A(H1N1)pdm09 viruses carrying the wild type gene, but it did not affect viruses bearing the NS1 C112A mutation. Thus, hsa-miR-1307-3p is a novel antiviral micro RNA targeting H1N1 NS1 protein, which might be exploited for the development of novel antiviral therapies.

2. Materials and methods

2.1. Gene sequencing

Virus RNA extracted from respiratory samples (NPS, TNAS, BAL) was amplified using a in house H1N1v-specific primer set to obtain the complete sequence of NS1 gene (Campanini et al., 2010). Purified PCR products were sequenced using the BigDye Terminator Cycle-Sequencing kit (Applied Biosystems, Foster City, USA) in an ABI Prism 3130xl Genetic Analyzer (Applied Biosystems, Foster City, USA). Sequences were assembled using the Sequencher software, version 4.6 (Gene Codes Corporation, Ann Arbor, USA).

The 2010-11 sequences analysed in this study were deposited with GenBank, National Center for Biotechnology Information (NCBI) (http://www.ncbi.nlm.nih.gov) with the GenBank accession numbers: **MF600315-MF600425**.

2.2. Cell lines

A549 (lung adenocarcinoma) cell line was grown at 37 °C and 5% CO_2 in Kaighn's Modification of Ham's F-12 Medium (F–12K) (Gibco), supplemented with 10% fetal bovin serum (Lonza) and 1% gentamicin. Stable clones A549 miR-1307 and A549 scrambled were grown at 37 °C and 5% CO_2 in F–12K, supplemented with 10% fetal bovin serum, 1% gentamicin and 2 μg/ml puromycin (Sigma-Aldrich).

2.3. Generation of A549 miR-1307 and A549 stable cell clones

To increase the expression of hsa-miR-1307-3p, the pEZX-MR04 vector encoding for the pre-miR-1307 was used (GeneCopoeia) and the scrambled control vector. A549 cell line was grown on 10 cm dishes to 80% confluency and then the cells were transfected with ViaFect (Promega) tranfection reagent following the manufacturer's protocol using 4 μg of both vectors. Following 24 h after transfection cells were split using 1:10 dilution/dish and incubated for further 24 h before the start of the selection. The selective concentration of puromycin was 2 μg/ml. After 2 weeks of selection process, clones were picked using sterile cloning discs (Sigma-Aldrich), and they were grown in F–12K medium containing 2 μg/ml puromycin.

2.4. Infectivity assays

Viral isolates VR 10137, bearing C112 NS1 (wild type) protein, and VR 10143 (mutant), bearing C112A NS1, of influenza A/H1N1/2009 isolated in 2011 from nasal swabs of two patients with upper respiratory symptoms were used for viral infections. Viruses were propagated in MDCK (Madin-Darby canine kidney) cell and seven days after inoculum viruses were collected and centrifuged for 10 min 2500 rpm to obtain cell free supernatant. A 1:50 dilution was chosen for the wild type and 1:60 for the mutant to obtain the same amount of virus that was 4×10^4 copies/ml.

200 μl of the two viral isolates: VR 10137 (wild type) and VR 10143 (mutant) at the established working dilution were inoculated into A549 scrambled cells and A549 miR-1307 shell vials previously prepared. The inoculated shell vials were centrifuged for 30 min at 1800 rpm and incubated at 33 °C 5% CO_2. After 2 h the inoculum was removed, cells were washed 5 times in F12K serum free medium and 2 ml of the same medium plus 5γ/ml trypsin was added. For quantitative qRT-PCR, after 72 h supernatant was collected and tested, following the protocol of qRT-PCR for influenza A(H1N1) of WHO Collaborating Centre for influenza at CDC Atlanta, United States of America (http://www.who.int/csr/resources/publications/swineflu/realtimeptpcr/en/). For infected cells counting, after 72 h medium was removed and cells were fixed in methanol/acetone (2/1) for 10 min. Cell monolayer was stained with influenza A virus specific monoclonal antibody directly conjugated with fluorescein (Flua DFA reagent Light Diagnostics (Chemicon) Millipore - Merck (Kenilworth, NJ 07033 U.S.A.)). Positive infected fluorescent cells were counted with a fluorescent microscope at 20X.

2.5. IFN-α treatment

The lyophilized IFN-α (Sigma-Aldrich) was reconstituted in sterile ddH$_2$O to final concentration of 0.1 mg/ml. On day 1, 10×10^4 A549 cells were plated in a 6 well dishes plate and incubated 37 °C and 5% CO_2 in F–12K medium O/N. On day 2, 250U/ml IFN-α were added to the medium and cells were then harvested at 24 h, 48 h and 72 h post treatment for RNA extraction and qRT-PCR analysis.

2.6. RNA isolation, reverse transcription and qRT-PCR

2.6.1. Hsa-miR-1307-3p
RNA extraction was performed using ReliaPrep RNA Cell Miniprep System (Promega). Reverse transcription of total RNA and qRT-PCR for the detection of hsa-miR-1307-3p expression were performed using the All-in-One miRNA qRT-PCR Reagent Kit and All-in-One miRNA qPCR Primer for hsa-miR-1307-3p (Cat. no. HmiRQP0154) (GeneCopoeia) following the manufacturer's protocols. The U6 small nuclear RNA pseudogene of miScript Primer Assay (Qiagen) was used as reference gene. The amplification program was as follow: RNA pre-incubation (10 min at 95 °C); 45 cycles of amplification (10 s at 95 °C; 20 s at 60 °C; 10 s at 72 °C); cooling (30 s at 40 °C).

2.6.2. C112 and C112A NS1 genes
RNA extraction was performed using ReliaPrep RNA Cell Miniprep System (Promega). The M-MulV Reverse Transcriptase kit (Invitrogen) was used for reverse transcription of total RNA, following the manufacturer's protocol. The qRT-PCR reactions were performed using GoTaq qPCR Master Mix (Promega). The β-actin (*ACTB*) and glyceraldehyde-3-phosphate dehydrogenase (*GAPDH*) were used as reference genes. Primers for NS1 genes were purchase from Bio-Fab research and the sequences are the following: 5′-TTGCGTGCGATT GGAC-3′ for sense primer, and 5′-AAGCCCTTAGTAGTATCAAG-3′ for antisense primer. The amplification program was as follow: RNA pre-incubation (10 min at 95 °C); 40 cycles of amplification (10 s at 95 °C; 20 s at 60 °C; 10 s at 72 °C); cooling (30 s at 40 °C). All qRT-PCR reactions were carried out in the LightCycler 480 Instrument (Roche).

2.7. Gene lists enrichment analysis

Up- or downregulated gene lists were used to test enrichment of biological functions. To this aim, the DAVID v6.7 web-tool https://david.ncifcrf.gov (Huang et al., 2009a; Huang et al., 2009b); was used to test functional enrichment of Gene Ontology (GO) terms. Significant enrichments were selected by a threshold of 5×10^{-2} of Benjamini's corrected *p* values.

3. Results

3.1. Identification of natural polymorphisms of the H1N1 NS1 protein specific to the 2010-11 season

The sequences of the NS1 protein from 200 strains of the A(H1N1)

pdm09 IAV collected during epidemiological surveillance in the 2009–10 (n = 89) and 2010–11 (n = 111) epidemic waves in Italy, were aligned to the reference sequence of the A/California/04/2009(H1N1) strain. As expected, the NS1 genes showed very high sequence identity across the different strains, with few polymorphic variants. The few detected mutations were used to define different haplotypes, according to their presence in the individual strains. A polymorphism at position 112 (C112A), was detected in 1/89 and 54/111 strains from the 2009–10 and 2010-11 seasons, respectively. Another polymorphism at position 264 (C264T), was not detected in the 2009-10 season strains, whereas it was found in 31/111 strains from the 2010-11 season. These two mutations were never associated in the same viral strains, thus defining two separate haplotypes, named HB-5 and HD, respectively, which were predominant in the 2010-11 season (Table S1). Interestingly, HB-5 was the only haplotype circulating in both seasons.

3.2. Correlation of the haplotypes HD and HB-5 with clinical symptoms

The 200 viral strains were then stratified according to the severity of symptoms of the infected patients in three groups (for details see also Supplemental Information): ARDS (acute respiratory distress syndrome, n = 50); LRTI (lower respiratory tract viral dissemination, n = 60); URTI (upper respiratory tract viral infection, n = 90). As shown in Table 1 the C112A polymorphism showed strong association ($p < 0.02$) to the ARDS group, with respect to the URTI group, but only when the isolates of both seasons were included in the analysis. Considering only the 2010-11 seasonal samples (n = 111) the association of the C112A polymorphism with ARDS was not significant ($p = 0.08$). Unfortunately, it was not possible to increase the sample size, since in the following years (up to the 2016-17 seasonal epidemic), this polymorphism was not detected anymore. No statistically significant association with the ARDS cases was found for the C264T mutation in all cases.

3.3. Correlation of haplotype HB-5 in NS1 with mutations in the HA gene known to increase pathogenicity

Previous phylogenetic analysis of the HA gene of the same set of Italian strains, revealed two sites under positive selection during the 2010-11 season: D97N and D222 E/G. The mutation D222G has been linked to increased pathogenicity (Baldanti et al., 2011; Piralla et al., 2011; Goka et al., 2014). In our samples the D97N substitution was

present in 16/16 URTI strains and 17/19 ARDS strains bearing the NS1 C112A mutation. The D222G was present in 0/16 URTI and 3/19 ARDS strains bearing the NS1 C112A mutation. Another mutation, S202T, was present in 16/16 URTI strains and 19/19 ARDS strains bearing the NS1 C112A mutation. Other mutated HA positions which have been suggested to contribute to increased pathogenicity or antigenic variation of A(H1N1)pdm09 IAV, such as Q188, S190, N194, Q223, E224, were not found in any of the viral strains bearing the NS1 C112A substitution. Thus, no correlation was apparent between the presence of these polymorphisms in the HA gene together with the C112A mutation in the NS1, and the severity of symptoms.

3.4. The NS1 protein C112A polymorphism falls within the putative target site of a human microRNA

The two NS1 mutations identified were synonymous, affecting codons 38 and 88, respectively (C*G*A - > A*G*A; CG*C* - > CG*U*), without changing the amino acid sequence (Arg - > Arg). A bioinformatic analysis performed on the NS1 coding sequence (CDS) of different isolates, either carrying the NS1 wild type or with the C112A or C264T mutations, identified the human miRNA hsa-miR-1307-3p as the strongest interactor of wild type NS1, but detected a much weaker binding to the C112A NS1 mutant (below the free energy threshold set at −20 kcal/mol) (Fig. 1 A - B, Table S2). Sequence alignment showed that the C112A mutation introduced a mismatch in the seed region of the miRNA (Fig. 1 C), changing a C:G base pair into A:G. No miRNA was predicted to be affected by the C264T mutation (data not shown). A BLAST search confirmed that the target sequence for hsa-miR-1307-3p was not present in other portions beside the NS1 gene of the eight gene segments of H1N1 IAV isolates present in the Influenza Research Database. Target sites for miRNAs have been detected in the CDS of many human genes (Lee and Gorospe, 2011; Reczko et al., 2012; Guojing et al., 2015) and two *Sus scrofa* miRNAs have been shown to downregulate the swine SIV–H1N1/2009 HA and NS1 proteins by binding to their CDS (Zhang et al., 2017). Thus, we next tested the ability of hsa-miR-1307-3p to downregulate wild type and the C112A mutant NS1.

3.5. Construction of A549 model cell line for stable miR-1307 overexpression

We generated a clone of the human lung alveolar cells adenocarcinoma A549 cell line, stably overexpressing the hsa-miR-1307-3p in the pEZX-MR04 expression vector with fluorescent protein eGFP as a reporter gene under the control of the CMV promoter. Cells expressing eGFP were detected by fluorescent microscopy and the expression of hsa-miR-1307-3p was confirmed by RT-qPCR. As shown in Fig. 2 A the levels of hsa-miR-1307-3p in the A549 stable clone were 10-fold higher than the endogenous expression of this miRNA in the control clone carrying the scrambled sequence.

3.6. Overexpression of hsa-miR-1307-3p reduces NS1 expression and viral replication of wild type H1N1 virus, but not of the NS1 C112A mutant

Next, we performed infection of either A549 scrambled or A549 miR-1307 cell lines, with the A(H1N1)/2011/VR10143 viral isolate carrying the C112A mutation in NS1, or the A(H1N1)/2011/VR10137 viral isolate carrying wild type NS1. Both were clinical strains coming from the 2010-11 season and sampled in the same area of northern Italy (Lombardy). At 72 h post-infection, the viral titre, measured as number of genome copies as detected by qRT-PCR, carrying the wild type NS1 were 3-fold less in the A549 miR-1307 cells supernatant, than with the same virus infecting the A549 scrambled cells (Fig. 2 B). On the other hand, there was not a significant decrease of viral replication in A549 miR-1307 infected with the virus carrying the C112A NS1 protein, with respect to the A549 control cells (Fig. 2 B). Similarly, the H1N1 strain carrying the wild type NS1 resulted in a 7- fold lower number of

Table 1
Frequencies and statistical analysis of the NS1 C112A and C264T polymorphisms among the different H1N1 isolates grouped according to the corresponding clinical symptoms.

	ARDS[a]	LRTI	URTI	Tot
C112A				
n_{C112A}	19	19	16	54
n_{wt}	31	41	74	146
n_{tot}	50	60	90	200
$f_{(C112A)}$[b]	0.380	0.317	0.178	0.270
χ^2 *p value*[c]	0.008	0.049		
C264T				
n_{C264T}	10	13	8	31
n_{wt}	40	47	82	169
n_{tot}	50	60	90	200
$f_{(C264T)}$[b]	0.200	0.217	0.089	0.155
χ^2 *p value*[c]	0.060	0.027		

[a] ARDS, acute respiratory distress syndrome; LRTI, low respiratory tract infection; URTI, upper respiratory tract infection.

[b] Observed frequencies of the polymorphisms, $f = n_{mut}/n_{tot}$.

[c] Chi-square *p*-value of the observed frequencies in the ARDS and LRTI groups in comparison with the URTI group. Significance was set at $p < 0.02$.
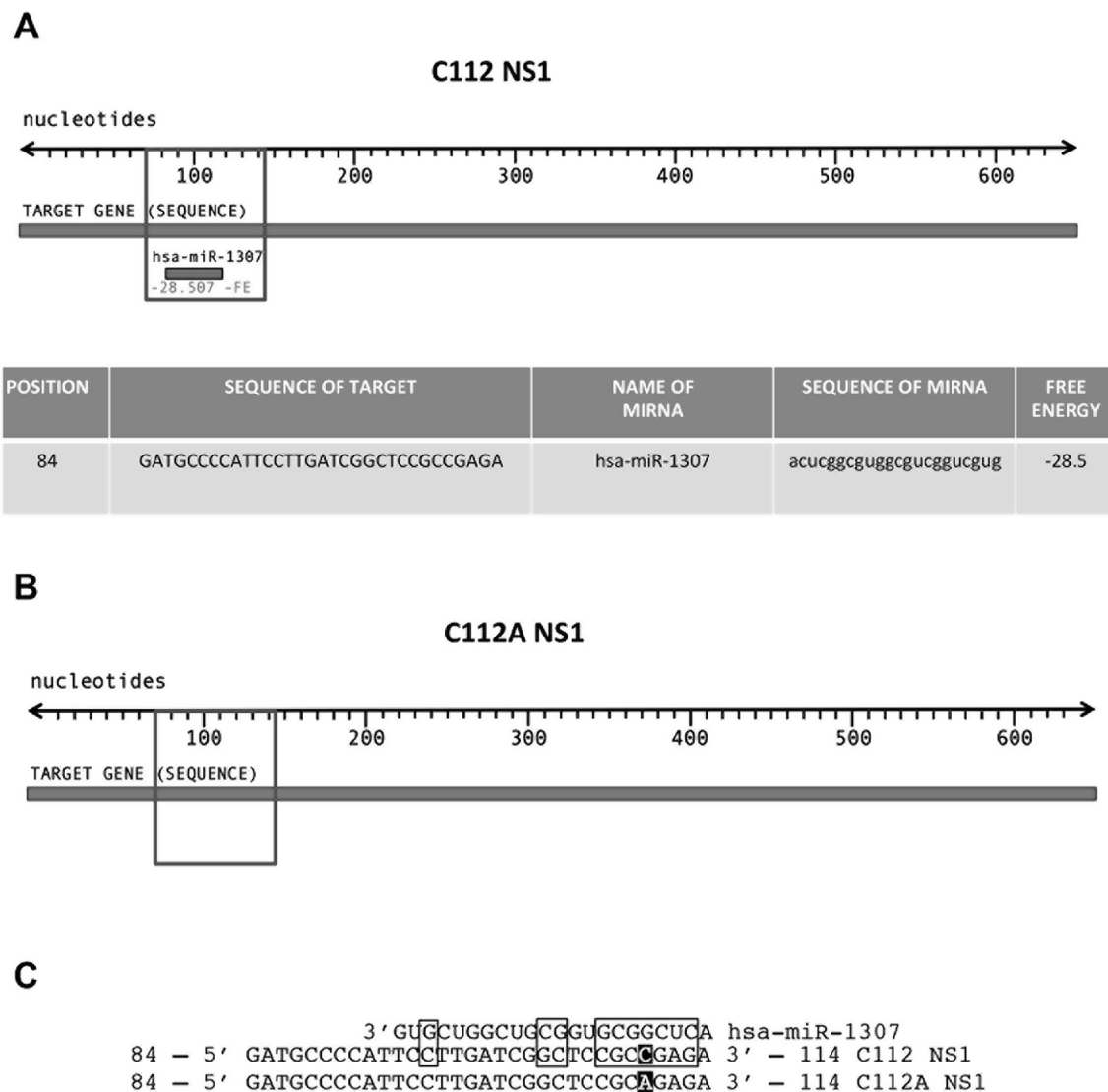
Fig. 1. Bioinformatic analysis of miRNAs targeting NS1. (A) Predicted hsa-miR-1307-3p miRNA interaction with C112 NS1 according to the web-based tools MicroInspector (http://bioinfo1.uni-plovdiv.bg/cgi-bin/microinspector/) and IntaRNA (http://rna.informatik.uni-freiburg.de/IntaRNA/Input.jsp). (B) As in panel A but with the mutated C112A NS1. (C) Sequence of hsa-miR-1307-3p aligned to its predicted target C112 NS1 sequence. The regions of complementarity are boxed. The position of the C112A single point mutation is highlighted.

infected cells in the A549 miR-1307 cell line, with respect to the A549 scrambled control cells, while no difference was observed in the number of infected cells by the virus carrying the C112A NS1 mutant protein between the two cell lines (Fig. 2 C). Accordingly, as shown in Fig. 2 D, the levels of wild type NS1 transcripts upon infection were 2-fold less in A549 stably expressing hsa-miR-1307-3p, compared to the A549 scrambled cell line. On the other hand, the levels of the C112A mutant NS1 transcripts in A549 miR-1307 cells were similar, or even superior, to those detected in A549 control cells. These results indicated that overexpression of hsa-miR-1307-3p is able to reduce wild type NS1 expression and viral replication in infected cells, but does not affect the C112A NS1 mutant. As shown in Fig. S1 and Table S3, the NS1 genes of these two isolates differ only at the nucleotide position 278 (278 A for VR-10137 and 278G for VR-10143) and 112 (112C for VR-10137 and 112 A for VR-10143). Each of the two strains also differ in the NS1 gene form the reference strain A(H1N1)pdm09/Texas/04/2009, at two positions only (Table S3). TheVR-10143 strain had the wild type sequence at position 278 (G278), while the VR-10137 had the wild type sequence at position 112 (112C). Both isolates carried an additional polymorphism with respect to the reference strain at position 367 (A367G).

Thus, the different ability of hsa-miR-1307-3p to suppress the expression of NS1 for the two strains could be ascribed solely to the presence of the C112A mutation (Table S3). Overall, the nucleotide identity between the NS1 genes of the two isolates was 99.7%. Sequencing of the two isolates across the most variable regions of IAV genomes, the HA and NA genes, revealed nucleotide identities of 98.9% and 99.2%, respectively (Fig. S2).

3.7. H1N1 IAV carrying the NS1 C112A mutation replicates better than wild type in A549 cells

Since A549 cells express endogenous levels of hsa-miR-1307-3p, we assessed the levels of ectopically expressed NS1 either wild type or carrying the C112A mutation. As shown in Fig. 3 A, the expression of wild type NS1, as judged by Western blot, was greatly reduced with respect to the levels observed for the NS1 C112A mutated protein. Next, cells were infected with the A(H1N1)/2011/VR10143 strain carrying the C112A mutation in NS1, or the A(H1N1)/2011/VR10137 strain carrying wild type NS1. As shown in Fig. 3 B, the virus carrying the NS1 C112A mutation, replicated 2- fold better in A549 cells than the wild
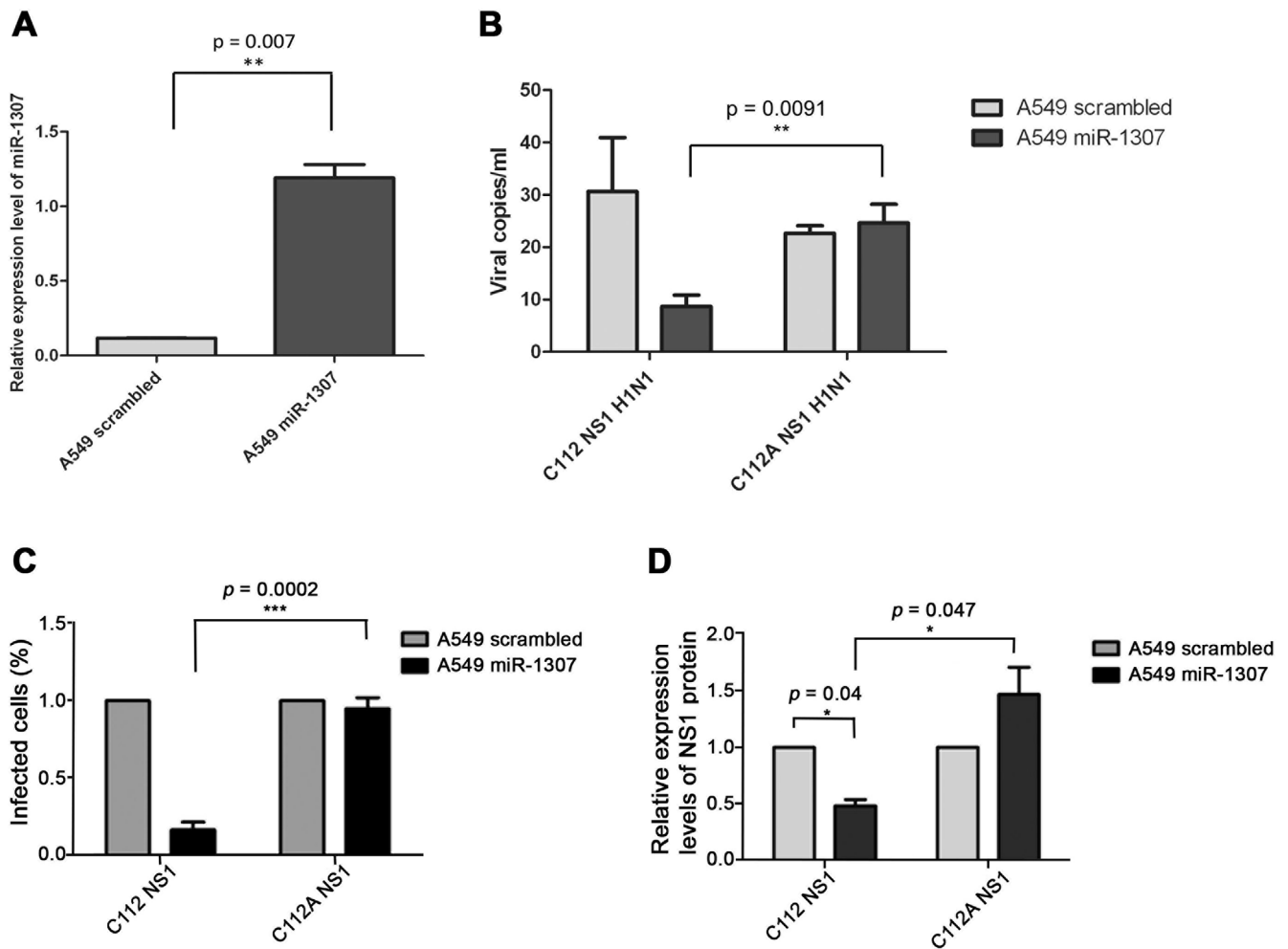
Fig. 2. Effects of hsa-miR-1307 overexpression in A549 cells on NS1 expression and virus replication. Error bars are ± S.D. for three independent replicates. Statistical significance was assessed with Student's *t*-test. The corresponding *p* values are shown on top of the bars. **A.** Level of hsa-miR-1307 quantified by RT-qPCR in A549 scrambled control (grey bar) and A549 stable clone expressing miR-1307 (dark grey bar). Values obtained by RT-qPCR were normalized with GAPDH gene as internal control. **B.** Replication efficiency defined as viral genome copies/ml after infection with the strains VR 10143 carrying C112A NS1, and VR 10137 carrying C112 NS1, in A549 miR-1307 (dark grey bars) or A549 scrambled control cells (light grey bars). Values obtained by qRT-PCR were normalized with GAPDH gene as internal control. **C.** Replication efficiency defined as number of infected cells after infection with the strains VR 10143 carrying C112A NS1, and VR 10137 carrying C112 NS1, in A549 miR-1307 (dark grey bars) or A549 scrambled control cells (light grey bars). Values obtained are represented as relative with respect to A549 scrambled control cells. **D.** Comparison of relative expressions of C112 NS1 and C112A NS1 in A549 miR-1307 (dark grey bars) and A549 scrambled control (light grey bars) cells after viral infection. Values of expression levels of both NS1 proteins obtained by qRT-PCR were normalized with GAPDH gene as internal control and represented as relative values with respect to A549 scrambled control cells.

type, as judged by the number of viral genome copies detected in the supernatant. Thus, endogenous expression of hsa-miR-1307-3p in A549 cells can reduce replication of the H1N1 IAV carrying wild type NS1, but not of the viruses bearing the NS1 C112A mutation. To directly assess the effects of hsa-miR-1307-3p levels on NS1 expression, we assessed the mRNA levels of ectopically expressed NS1 either wild type or carrying the C112A mutation in the A549 scrambled cell line or A549 stably expressing hsa-miR-1307-3p cells. As shown in Fig. 3 C, the relative levels of C112A mutant proteins with respect to wild type NS1 were 3- fold higher in cells overexpressing hsa-miR-1307-3p, confirming that the miRNA was directly targeting NS1 and that in the presence of hsa-miR-1307-3p, the C112A NS1 expression was favoured over C112 (wild type) NS1.

3.8. Transcription of the hsa-miR-1307-3p gene is repressed by IAV infection but triggered by interferon α

The levels of endogenous miR-1307-3p expression were measured in A549 cells by qRT-PCR at 72 h p. i. with the A(H1N1)/2011/VR10137

strain carrying wild type NS1. As shown in Fig. 3 D, miR-1307-3p was repressed upon viral infection, with respect to uninfected cells. Cellular miRNA downregulation is often associated to IAV infections and might be correlated to viral pathogenicity (Makkoch et al., 2016; Gao et al., 2017; Khongnomnan et al., 2018; Poore et al., 2018). However, even in the presence of repression by the virus, miR-1307-3p endogenous levels are sufficient to reduce viral replication, albeit to a lower extent with respect to A549 cells overexpressing miR-1307-3p (compare Fig. 3 B with Fig. 2 B). Interferons (IFNs) are produced as part of the innate immune response against viral infections. Wild type A549 were treated with IFN-α at 250U/ml. Cells were collected at 24 h, 48 h and 72 h post-treatment followed by RNA extraction. Relative expression levels of hsa-miR-1307-3p in IFN-treated *vs.* untreated cells, were detected by qRT-PCR. As shown in Fig. 3 E, hsa-miR-1307-3p expression started to increase at 24 h post IFN-α treatment, peaked at 48 h and then returned to basal levels at 72 h. At 48 h post-treatment the hsa-miR-1307-3p levels were 4- fold higher than at 24 h. These data suggested that the hsa-miR-1307-3p is part of the IFN type I - controlled innate immune response.
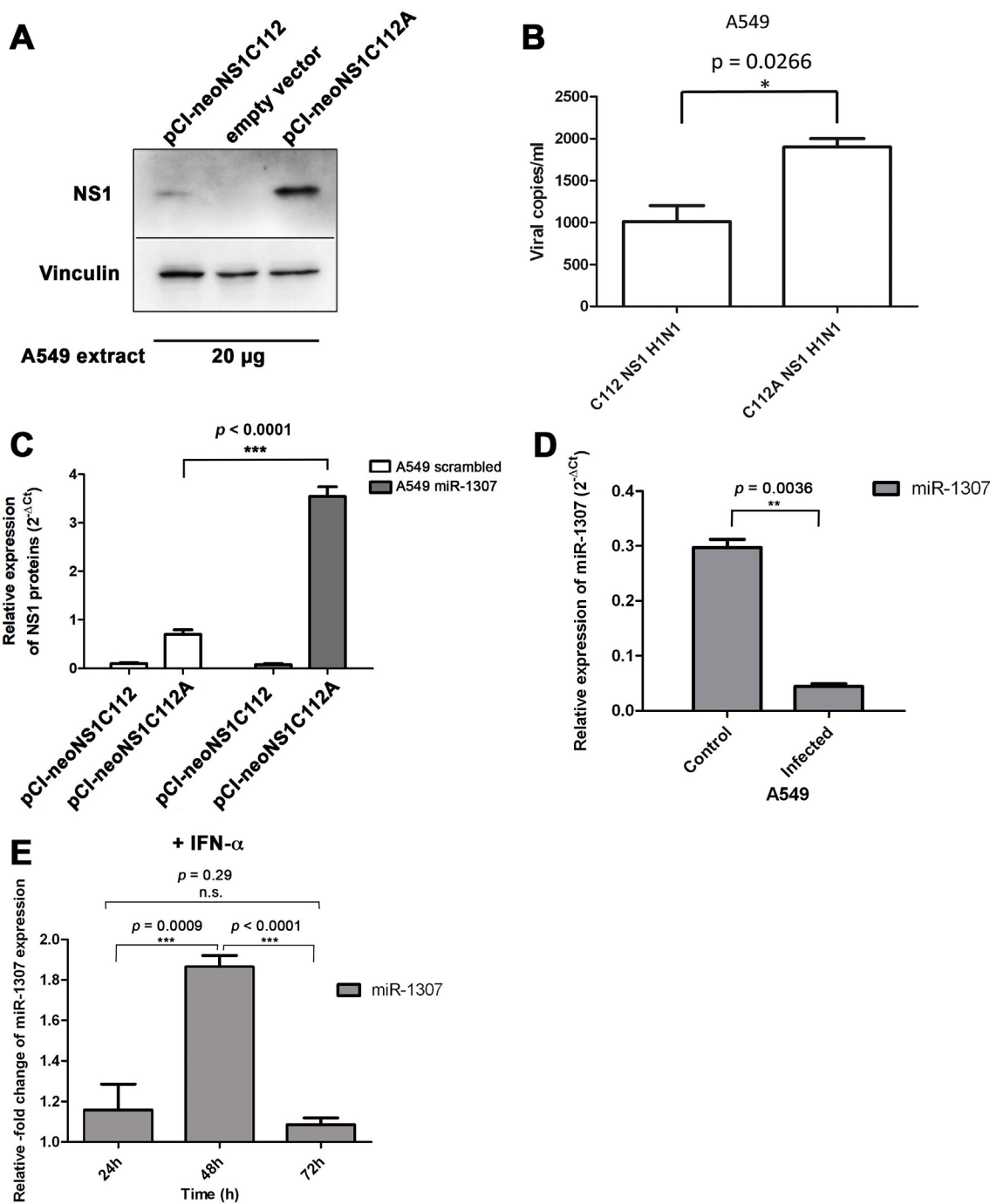
Fig. 3. Levels of NS1 expression and virus replication in the presence of endogenous hsa-miR-1307 in A549 cells and effects of IFN-α. A. Western blot analysis of A549 cells transfected with plasmids expressing either the wild type (pCI-neoNS1C112) or mutated (pCI-neoNS1C112A) NS1 protein. The black line indicates that the image shows two different portions of the membrane. The membrane was cut in half and each part separately incubated with rabbit polyclonal anti-NS1 antibody (top lane), or mouse monoclonal anti-vinculin antibody (bottom lane), respectively, for the detection of the corresponding proteins. C, negative control (empty vector transfected A549 cells). **B**. Replication efficiency defined as viral genome copies/ml after infection with VR 10143 carrying C112A NS1, and VR 10137 carrying C112 NS1, in A549 wild type cells. Values obtained by qRT-PCR were normalized with GAPDH gene as internal control. **C**. Relative NS1 mRNA levels in A549 control cells (white bars) or overexpressing hsa-miR-1307 (grey bars), transfected with plasmids expressing either the wild type (pCI-neoNS1C112) or mutated (pCI-neoNS1C112A) NS1 protein. Values obtained by qRT-PCR were normalized with GAPDH gene as internal control. **D**. Endogenous hsa-miR-1307 expression levels were measured at 72 h in A549 uninfected or IAV infected cells. Values are the mean of two replicates. Error bars are ± S.D. Student's t-test *p* value is indicated on top. **E**. Increasing levels of hsa-miR-1307 after IFN-α treatment. Relative expression of miR-1307 was measured by qRT-PCR in the A459 cell line at 24 h, 48 h and 72 h after treatment with 250U/ml of IFN-α, normalized with GAPDH and β-actin genes as internal controls and expressed as relative -fold change with respect to untreated cells. Student's t-test *p* values are indicated on top.
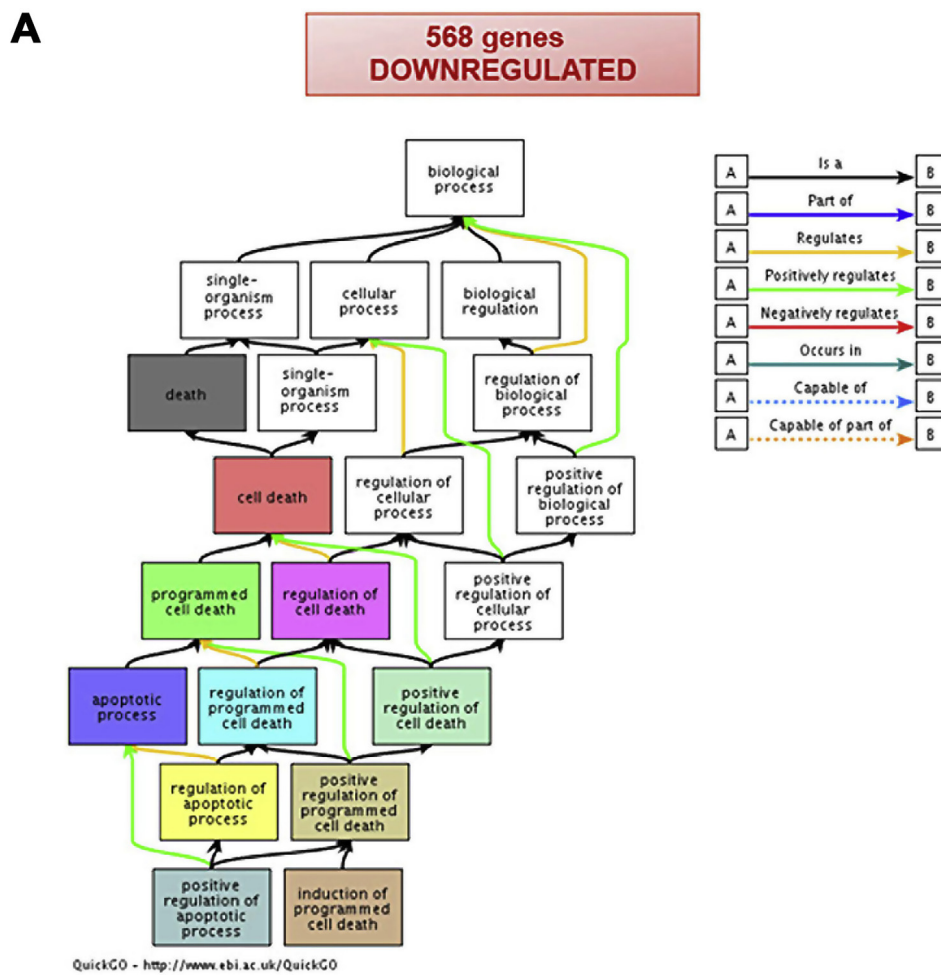
A

Fig. 4. hsa-miR-1307 downregulates genes involved in different molecular pathways A. Genes experimentally found downregulated by overexpression of hsa-miR-1307-3p in A549 cells are grouped according to their respective biological processes. Image generated from the microarray analysis data with QuickGO (http://www.ebi.ac.uk/QuickGO). **B.** Western blot analysis of p21 expression in A549 miR-1307 and A549 scrambled control cells. p21 signal intensities were normalized to the actin control. The relative ratio of normalized values for miRNA overexpressing cells with respect to controls for each crude extract total protein concentration is indicated below the panel. All samples were transferred to the same membrane. The different portions of the membrane were mounted separately in the image for better clarity.

B
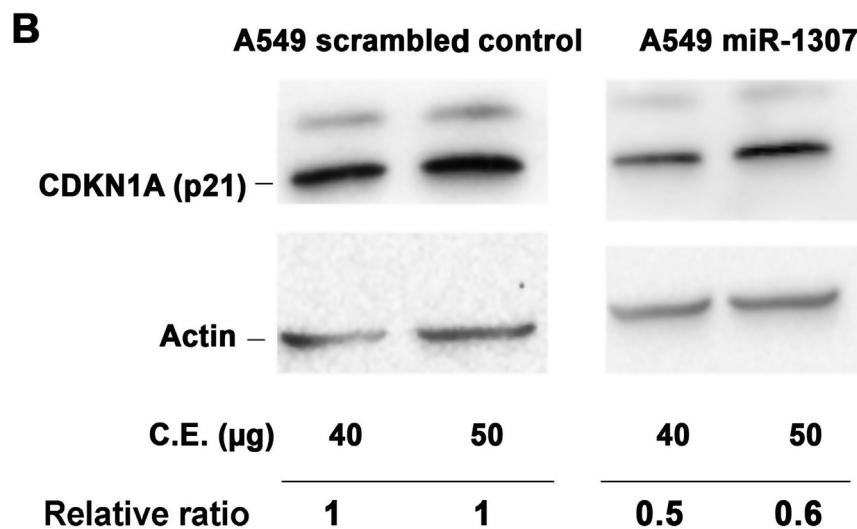
3.9. Genome-wide analysis of hsa-miR-1307-3p regulated genes

In order to gain a better understanding of the genes regulated by hsa-miR-1307-3p, we performed a microarray analysis on A549 miR-1307 and A549 scrambled cell lines. Overexpression of hsa-miR-1307-3p resulted in 696 genes upregulated and 568 genes downregulated, respectively, when compared to A549 control cells. A Gene Ontology (GO) enrichment analysis was carried out by the web-tool DAVID (https://david.ncifcrf.gov), in order to organize these genes according to their respective Biological Process (BP), Cellular Component (CC), and Molecular Function (MF) classes. The Benjamini correction for multiple testing with a significance threshold of q-value $< 1 \times 10^{-2}$, was used. The GO analysis indicated that the majority of upregulated genes encode for proteins involved in DNA replication, DNA repair and cellular response to stress. The genes downregulated by hsa-miR-1307-3p turned out to be mainly involved in the regulation of apoptosis, as

indicated by the BP analysis (Fig. 4A). One prominent cell cycle and apoptosis regulating gene identified as downregulated in the analysis was *CDKN1*, encoding the cyclin dependent kinases inhibitor p21. Western bot analysis confirmed its downregulation in A549 cells over-expressing hsa-miR-1307-3p, with respect to A549 control cells (Fig. 4 B). The genes ranked as most significantly downregulated by the microrray analysis, are listed in Table S4, along with their respective functions. 30 genes out of 45 (66.6%) matched also those predicted by bioinformatic analysis as putative targets of hsa-miR-1307-3p. Among them 15 (50%) regulate cell proliferation and apoptosis, mostly in a positive fashion, 7 (23%) were involved in the regulation of the inflammatory and IFN response, while the remaining 8 (27%) were involved in the regulation of various metabolic pathways.

4. Discussion

Hundreds of cellular miRNAs are differentially expressed upon IAV infection (Ma et al., 2016; Gao et al., 2019) and some also specifically target IAV proteins, such as NP, PB1, PB2, PA, and NA (Nguyen et al., 2018; Kumar et al., 2018; Gao et al., 2019; Jiao et al., 2019). However, to the best of our knowledge, no human miRNA has been validated so far as a suppressor of the IAV NS1 protein expression. In this study, we have provided evidence that the human hsa-miR-1307-3p limits IAV replication by targeting the viral protein NS1.

The gene encoding the human miRNA hsa-miR-1307 is located on chromosome 10, in the intron region of the USMG5 gene. The hsa-miR-1307 transcript was originally found selectively expressed in Epstein-Barr virus induced nasopharyngeal carcinomas (Zhu et al., 2009) and other studies suggested its role in cancer progression (Zhou et al., 2015; Chen et al., 2017; Qiu and Dou, 2017; Wang and Zhu, 2018), but its actual cellular targets and physiological functions are still poorly known. Our microarray analysis indicated a role of hsa-miR-1307-3p in promoting cell proliferation and inhibiting apoptosis. The NS1 protein of H1N1 IAV has been shown to prevent cell cycle progression through S-phase and mitosis, providing a more favourable cellular environment for viral replication (Jiang et al., 2013). Thus, it could be hypothesized that by targeting NS1 and promoting cell proliferation, hsa-miR-1307-3p might counteract the cell cycle and gene expression block caused by IAV infection. The down regulation of hsa-miR-1307-3p upon viral infection might be a first mechanism of viral evasion from the innate immune response. Indeed, hsa-miR-1307-3p appears a regulator of several genes of the innate immune response pathway. Our result suggest that hsa-miR-1307-3p is induced by type I IFN, which thus potentially counteracts its repression caused by the virus. This hypothesis will require further studies to be tested, also analyzing the effect of hsa-miR-1307-3p in a broader panel of human airway epithelial cell lines. In this study we have used two clinical isolates derived from the same season and geographical area. We believe that using field circulating vs. laboratory IAV strains would more accurately reflect the situation in nature. The two clinical isolates used in this study were highly similar, with a mean nucleotide identity assessed through three gene segments (NA, HA, NS1) > 99%. The target sequence of hsa-miR-1307-3p was not present anywhere in their genomes besides on the NS1 gene segment. In addition, both isolates replicated with similar efficiency in A549 cells, while the strain carrying the C112A NS1 was favoured only in the presence of high hsa-miR-1307-3p expression. We cannot exclude that mutations on other genes than NS1 might affect viral infectivity and/or replication kinetics of the two isolates. However, it is highly unlikely that mutations in genes not targeted by hsa-miR-1307-3p would confer an advantage only in response to an increase in the levels of such specific miRNA, as observed in the case of the C112A mutation in the miRNA target sequence of the NS1 gene.

The frequency of the C112A mutant strains circulating in Italy during the season 2010–11 was quite high (27.9% of the total H1N1 clinical samples examined). This, and the fact that it belonged to a separate haplotype, suggest that it was introduced by a founder virus

during the pandemic and subsequently spread locally. A BLAST search of the Influenza Research Database (www.fludb.org) using the hsa-miR-1307-3p NS1 binding site, revealed only 144 strains bearing the C112A mutation, with a peak in the 2010-11 season (Table S5). Thus, it seems that this mutation became fixed in a small fraction of worldwide circulating influenza strains in the 2010–11, but rapidly disappeared in the subsequent seasons. This fact, together with its relative low frequency, at least as qualitatively estimated from the number of mutant strains with respect to the total isolates in the database, both suggest that the viral mutants were outcompeted by other circulating H1N1 strains. Whether it was due to an excessive pathogenicity, which limited the chances of inter-human transmission, or by other factors, it is presently not known. However, the C112A polymorphism has been detected also in swine IAV strains of the H1N1, H3N2 and H1N2 subtypes (Table S5), suggesting circulation of this mutation in the swine reservoir, with the potential of being transferred back by genetic reassortment to human IAV strains.

5. Conclusions

In recent years, increasing attention has been focused on potential therapeutic strategies against IAV infections based on manipulation of cellular miRNAs. For example, delivery of antiviral miRNAs by lentiviral vectors has been shown to inhibit IAV replication in infected cells (Xu et al., 2015). Similarly, engineered IAV particles that express exogenous miRNA sequences can be used to generate attenuated strains for novel vaccines (Zhang et al., 2015 Aug; Izzard et al., 2017). The results presented here, identifying both a target sequence in the NS1 gene and the corresponding antiviral miRNA, can be exploited for the development of novel antiviral strategies.

Conflicts of interest

The authors declare that they have no financial or non-financial competing interests.

Data statement

The raw data supporting this paper are fully available from the authors.

6. Acknowledgments

Appendix A. Supplementary data

Supplementary data to this article can be found online at https://doi.org/10.1016/j.antiviral.2019.104593.

References

Baldanti, F., Campanini, G., Piralla, A., Rovida, F., Braschi, A., Mojoli, F., Iotti, G., Belliato, M., Conaldi, P.G., Arcadipane, A., Pariani, E., Zanetti, A., Minoli, L., Emmi, V., 2011. Segregation of virulent influenza A(H1N1) variants in the lower respiratory tract of critically ill patients during the 2010-2011 seasonal epidemic. Clin. Microbiol. Infect. 17, 1166–1169.

Belanov, S.S., Bychkov, D., Benner, C., Ripatti, S., Ojala, T., Kankainen, M., Kai Lee, H., Wei-Tze Tang, J., Kainov, D.E., 2015. Genome-wide analysis of evolutionary markers of human influenza A(H1N1)pdm09 and A(H3N2) viruses may guide selection of vaccine strain candidates. Genome Biol Evol 7, 3472–3483.

Campanini, G., Piralla, A., Paolucci, S., Rovida, F., Percivalle, E., Maga, G., Baldanti, F., 2010. Genetic divergence of influenza A NS1 gene in pandemic 2009 H1N1 isolates

with respect to H1N1 and H3N2 isolates from previous seasonal epidemics. Virol J 7, 209.

Chen, W.T., Yang, Y.J., Zhang, Z.D., An, Q., Li, N., Liu, W., Yang, B., 2017. MiR-1307 promotes ovarian cancer cell chemoresistance by targeting the ING5 expression. J. Ovarian Res. 10, 1.

Clark, A.M., Nogales, A., Martinez-Sobrido, L., Topham, D.J., DeDiego, M.L., 2017. Functional evolution of influenza virus NS1 protein in currently circulating human 2009 pandemic H1N1 viruses. J. Virol. 91 e00721-17.

Gao, S., Li, J., Song, L., Wu, J., Huang, W., 2017. Influenza A virus-induced down-regulation of miR-26a contributes to reduced IFNα/β production. Virol. Sin. 32, 261–270.

Gao, J., Gao, L., Li, R., Lai, Z., Zhang, Z., Fan, X., 2019. Integrated analysis of microRNA-mRNA expression in A549 cells infected with influenza A viruses (IAVs) from different host species. Virus Res. 263, 34–46.

Gasparini, R., Bonanni, P., Amicizia, D., Bella, A., Donatelli, I., Cristina, M.L., Panatto, D., Lai, P.L., 2013. Influenza epidemiology in Italy two years after the 2009-2010 pandemic: need to improve vaccination coverage. Hum. Vaccines Immunother. 9, 561–567.

Goka, E.A., Vallely, P.J., Mutton, K.J., Klapper, P.E., 2014. Mutations associated with severity of the pandemic influenza A(H1N1)pdm09 in humans: a systematic review and meta-analysis of epidemiological evidence. Arch. Virol. 159, 3167–3183.

Guojing, L., Zhang, R., Xu, J., Wu, C.I., Lu, X., 2015. Functional conservation of both CDS- and 3'-UTR-located microRNA binding sites between species. Mol. Biol. Evol. 32, 3276.

Huang, dW., Sherman, B.T., Lempicki, R., 2009a. Bioinformatics enrichment tools: paths toward the comprehensive functional analysis of large gene lists. Nucleic Acids Res. 37, 1–13.

Huang, dW., Sherman, B.T., Lempicki, R.A., 2009b. Systematic and integrative analysis of large gene lists using DAVID bioinformatics resources. Nat. Protoc. 4, 44–57.

Izzard, L., Dlugolenski, D., Xia, Y., McMahon, M., Middleton, D., Tripp, R.A., Stambas, J., 2017. Enhanced immunogenicity following miR-155 incorporation into the influenza A virus genome. Virus Res. 235, 115–120.

Jiang, W., Wang, Q., Chen, S., Gao, S., Song, L., Liu, P., Huang, W., 2013. Influenza A virus NS1 induces G0/G1 cell cycle arrest by inhibiting the expression and activity of RhoA protein. J. Virol. 87, 3039–3052.

Jiao, H., Zheng, Z., Shuai, X., Wu, L., Chen, J., Luo, Y., Zhao, Y., Wang, H., Huang, Q., 2019. MicroRNA expression profiles from HEK293 cells expressing H5N1 avian influenza virus non-structural protein 1. Innate Immun. 25, 110–117.

Khongnomnan, K., Poomipak, W., Praianantathavorn, K., Saengchoowong, S., Pisitkun, T., Poovorawan, Y., Payungporn, S., 2018. Human MicroRNAs expression profiles in influenza B virus-infected cells based on illumina MiSeq platform. MicroRNA 7, 204–214.

Krug, R.M., 2015. Functions of the influenza A virus NS1 protein in antiviral defense. Curr Opin Virol 12, 1–6.

Kumar, A., Kumar, A., Ingle, H., Kumar, S., Mishra, R., Verma, M.K., Biswas, D., Kumar, N.S., Mishra, A., Raut, A.A., Takaoka, A., Kumar, H., 2018. MicroRNA hsa-miR-324-5p suppresses H5N1 virus replication by targeting the viral PB1 and host CUEDC2. J. Virol. 92 e01057-18.

Lee, E.K., Gorospe, M., 2011. Coding region: the neglected post-transcriptional code. RNA Biol. 8, 44–48.

Ma, Y., Ouyang, J., Wei, J., Maarouf, M., Chen, J.L., 2016. Involvement of host non-coding RNAs in the pathogenesis of the influenza virus. Int. J. Mol. Sci. 18, 39.

Makkoch, J., Poomipak, W., Saengchoowong, S., Khongnomnan, K., Praianantathavorn, K., Jinato, T., Poovorawan, Y., Payungporn, S., 2016. Human microRNAs profiling in response to influenza A viruses (subtypes pH1N1, H3N2, and H5N1). Exp. Biol. Med. 241, 409–420.

Neumann, G., Noda, T., Kawaoka, Y., 2009. Emergence and pandemic potential of swine-origin H1N1 influenza virus. Nature 459, 931–939.

Nguyen, T.H., Liu, X., Su, Z.Z., Hsu, A.C., Foster, P.S., Yang, M., 2018. Potential role of MicroRNAs in the regulation of antiviral responses to influenza infection. Front. Immunol. 9, 1541.

Otte, A., Marriott, A.C., Dreier, C., Dove, B., Mooren, K., Klingen, T.R., Sauter, M., Thompson, K.A., Bennett, A., Klingel, K., van Riel, D., McHardy, A.C., Carroll, M.W., Gabriel, G., 2016. Evolution of 2009 H1N1 influenza viruses during the pandemic correlates with increased viral pathogenicity and transmissibility in the ferret model. Sci. Rep. 6, 28583.

Pan, C., Cheung, B., Tan, S., Li, C., Li, L., Liu, S., Jiang, S., 2010. Genomic signature and mutation trend analysis of pandemic (H1N1) 2009 influenza A virus. PLoS One 5, e9549.

Piralla, A., Pariani, E., Rovida, F., Campanini, G., Muzzi, A., Emmi, V., Iotti, G.A., Pesenti, A., Conaldi, P.G., Zanetti, A., Baldanti, F., 2011. Severe influenza a task force. PLoS One 6, e28332.

Poore, G.D., Ko, E.R., Valente, A., Henao, R., Sumner, K., Hong, C., Burke, T.W., Nichols, M., McClain, M.T., Huang, E.S., Ginsburg, G.S., Woods, C.W., Tsalik, E.L., 2018. A miRNA host response signature accurately discriminates acute respiratory infection etiologies. Front. Microbiol. 9, 2957.

Qiu, X., Dou, Y., 2017. miR-1307 promotes the proliferation of prostate cancer by targeting FOXO3A. Biomed. Pharmacother. 88, 430–435.

Reczko, M., Maragkakis, M., Alexiou, P., Grosse, I., Hatzigeorgiou, A.G., 2012. Functional microRNA targets in protein coding sequences. Bioinformatics 28, 771–776.

Su, Y.C., Bahl, J., Joseph, U., Butt, K.M., Peck, H.A., Koay, E.S., Oon, L.L., Barr, I.G., Vijaykrishna, D., Smith, G.J., 2015. Phylodynamics of H1N1/2009 influenza reveals the transition from host adaptation to immune-driven selection. Nat. Commun. 6, 7952.

Wang, X., Zhu, J., 2018. Mir-1307 regulates cisplatin resistance by targeting Mdm4 in breast cancer expressing wild type P53. Thorac Cancer 9, 676–683.

Wang, C., Zhang, Y., Wu, B., Liu, S., Xu, P., Lu, Y., Luo, J., Nolte, D.L., Deliberto, T.J., Duan, M., Zhang, H., He, H., 2013. Evolutionary characterization of the pandemic H1N1/2009 influenza virus in humans based on non-structural genes. PLoS One 8, e56201.

Xu, F., Liu, G., Liu, Q., Zhou, Y., 2015. RNA interference of influenza A virus replication by microRNA-adapted lentiviral loop short hairpin RNA. J. Gen. Virol. 96, 2971–2981.

Zehender, G., Pariani, E., Piralla, A., Lai, A., Gabanelli, E., Ranghiero, A., Ebranati, E., Amendola, A., Campanini, G., Rovida, F., Ciccozzi, M., Galli, M., Baldanti, F., Zanetti, A.R., 2012. Reconstruction of the evolutionary dynamics of the A(H1N1)pdm09 influenza virus in Italy during the pandemic and post-pandemic phases. PLoS One 7, e47517.

Zhang, H., Tang, X., Zhu, C., Song, Y., Yin, J., Xu, J., Ertl, H.C., Zhou, D., 2015 Aug Aug. Adenovirus-mediated artificial MicroRNAs targeting matrix or nucleoprotein genes protect mice against lethal influenza virus challenge. Gene Ther. 22 (8), 653–662.

Zhang, S., Wang, R., Su, H., Wang, B., Sizhu, S., Lei, Z., Jin, M., Chen, H., Cao, J., Zhou, H., 2017. Sus scrofa miR-204 and miR-4331 negatively regulate swine H1N1/2009 influenza A virus replication by targeting Viral HA and NS, respectively. Int. J. Mol. Sci. 18, 749.

Zhou, Y., Wang, M., Wu, J., Jie, Z., Chang, S., Shuang, T., 2015. The clinicopathological significance of miR-1307 in chemotherapy resistant epithelial ovarian cancer. J. Ovarian Res. 8, 23.

Zhu, J.Y., Pfuhl, T., Motsch, N., Barth, S., Nicholls, J., Grässer, F., Meister, G., 2009. Identification of novel Epstein-Barr virus microRNA genes from nasopharyngeal carcinomas. J. Virol. 83, 3333–3341.